RAPID COMMUNICATIONS

PHYSICAL REVIEW B VOLUME 52, NUMBER 10 1 SEPTEMBER 1995-II

Magnetic anisotropies of aligned carbon nanotubes

O. Chauvet and L. Forro
Laboratoire de Physique des Solides Semicristallins, Département de Physique, Ecole Polytechnique Fédérale de Lausanne, 1015 Lausanne, Switzerland

W. Bacsa, D. Ugarte,* B. Doudin, and Walt A. de Heer
Institut de Physique Experimentale, Ecole Polytechnique Fédérale de Lausanne, 1015 Lausanne, Switzerland
(Received 10 April 1995)

Angle-dependent conduction-electron spin resonance and static magnetic-susceptibility measurements of bulk, aligned, and partially purified carbon nanotube films show anisotropies reflecting the anisotropic character of the tubes. The Pauli susceptibility (above 40 K) of the tubes corresponds to about 10^{18} spins/cm^3, consistent with a semimetal. The g factors and their anisotropies are temperature dependent. The intrinsic tube resistivity is approximately an order of magnitude lower than the dc resistivity of the films. Qualitative changes below 40 K in the resistivity, the spin susceptibility, the g factors, and their anisotropies give evidence for charge-carrier localization.

The physicochemistry of carbon has recently seen a vigorous revival with the discovery of fullerenes, nanotubes, and onions. Like graphite, these mesoscopic systems are essentially sp^2 bonded; however, the curvature and special symmetries cause important modifications when compared with planar graphite. For example, single sheet nanotubes are predicted to be either semiconductors or metals, with anomalous anisotropic magnetic properties.[1] However, few of these remarkable predictions have been experimentally tested. Here we present static susceptibilities and magnetic resonance measurements of aligned carbon nanotubes.[2,3]

The production of aligned nanotube films is described in Ref. 4. Briefly, nanotube-containing material, produced by Ebbesen and Ajayan's method,[3] is ultrasonically dispersed in ethanol, centrifuged to separate the tubes, and to remove larger carbon particles. To produce nanotube films, the tube suspension is drawn through a 0.2 μm pore ceramic filter leaving a uniform black deposit on the filter. The deposited material is transferred on a thin Teflon sheet by pressing the tube coated side of the filter on the plastic. The filter is lifted off thus exposing the surface which was facing the filter. Scanning electron microscopy reveals that the tubes are highly aligned perpendicular to the Teflon surface. In these studies we examined nanotubes with diameters $d=10\pm5$ nm (corresponding to about 10–20 concentric, cylindrical, graphitic sheets) and lengths on the order of 1 μm.[4]

The static-magnetic susceptibilities were measured from $T=4$–300 K using a SQUID magnetometer. Susceptibility measurements were made with the tubes aligned parallel $\chi_\parallel$ and perpendicular $\chi_\perp$ to the field (Fig. 1). The nanotubes are diamagnetic and anisotropic. The magnitudes of the susceptibilities increase with decreasing temperature. Our measurements of, nonaligned samples, after sonification and cengrifugation (now shown), agree with the orientational average $(2\chi_\perp+\chi_\parallel)/3$ of the aligned sample. In contrast, susceptibilities of unprocessed nanotube-containing samples (see also Ref. 5) are considerably larger than those of the treated samples (Fig. 1 and also Ref. 6), indicating that the diamagnetism is dominated by larger (including nontubular and network) structures. In particular, we suspect that large loops composed of sintered nanotubes are carriers of large diamagnetic currents,[7] with a strikingly different temperature behavior compared with the ultrasonically separated tubes.

For planar graphite at temperature $T=300$ K, the susceptibility along the c axis (perpendicular to the planes) is $\chi_c=22\times10^{-6}$ emu/g (due to induced diamagnetic currents circulating around the graphitic hexagons[8]), and is much larger than along the a,b axes (parallel to the planes); $\chi_{ab}=0.5\times10^{-6}$ emu/g.[8] We constructed a simple nanotube model consisting of planar graphite rolled in a tube. In this model $\chi_{\perp\,\mathrm{model}}=(\chi_c+\chi_{ab})/2$, and $\chi_{\parallel\mathrm{model}}=\chi_{ab}$. In striking contrast with observations $|\chi_{\perp\,\mathrm{model}}|\gg|\chi_{\parallel\mathrm{model}}|$; however, the orientational average[6] $(2\chi_{ab}+\chi_c)/3\approx\chi_c/3$ is rather close to the experimental $(2\chi_\perp+\chi_\parallel)/3$. The large $|\chi_\parallel|$ may be caused by ring currents around the tube axis,[6] and the reduced values of $|\chi_\perp|$ compared with $|\chi_{ab}|$ are likely due to curvature effects and differences in intercalation distances compared with planar graphite.[9]

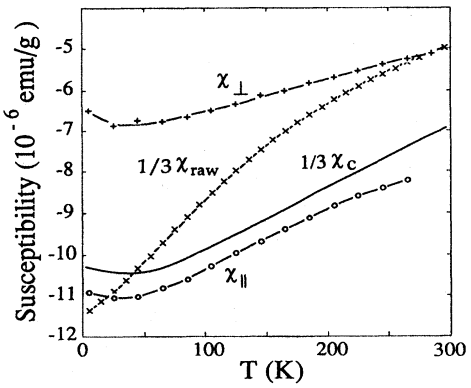

FIG. 1. Static magnetic susceptibility vs temperature. Nanotubes with the magnetic field perpendicular to the tubes (+); nanotubes with the field parallel to the tubes (○); unprocessed nanotube containing material (×); planar graphite, from Ref. 5 (– –).

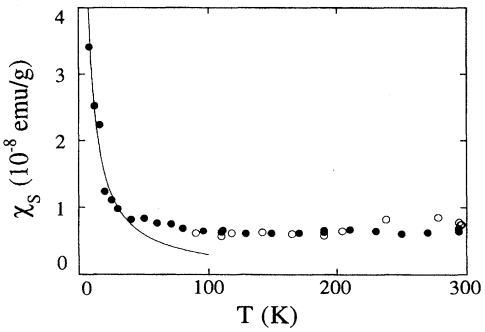

FIG. 2. Spin susceptibility of the carbon nanotubes vs temperature for $\theta=0°$(●) and 90°(○). For $T>40$ K, Pauli behavior is observed from an estimated 10^{18} carriers/cm^3 consistent with a semimetal. The low-temperature (<40 K) Curie tail (– –) represents 1.3×10^{18} localized spins/cm^3.

The ESR signals were measured at 9 GHz at temperatures from 4–300 K.[10] A wealth of information is obtained from the intensity, position, and shapes of the resonance lines. The sample can be rotated in the cavity to obtain orientational information. The ESR spectrum of the aligned carbon nanotubes (for a given angle θ of the tube axis with respect to the magnetic field B) consists of a single line over the entire temperature range. The line shape is Lorentzian above 40 K; below 40 K it becomes progressively asymmetric.[11] Besides the nanotube signal, a weak, narrow, isotropic Teflon signal ($g=2.0023$) is observed, whose position is temperature independent. This substrate signal serves as a marker and also allows monitoring of changes in the Q factor of the ESR cavity.

The spin susceptibility χ_s is derived from the ESR signal strength by numerical integration. Above 40 K (Fig. 2), we find a temperature-independent (Pauli) susceptibility $\chi_s=7\times10^{-9}$ emu/g. In comparison, for powdered graphite we find $\chi_s=2\times10^{-8}$ emu/g, consistent with reported values between 1 and 4×10^{-8} emu/g.[12,13] Pauli behavior indicates that the aligned nanotubes are metallic or semimetallic. For free electrons the Pauli susceptibility is given by $\chi=\mu_B^2N(E_F)$, where μ_B is the Bohr magneton and $N(E_F)$ is the density of states at the Fermi level. For our samples we find $N(E_F)=2.5\times10^{-3}$ states/eV/atom. This density of states is comparable to that of graphite.[14] Estimating the carrier concentration n given by $n=N(E_F)*E_F$ and taking for the Fermi energy E_F that of graphite (200 K) gives $n\sim4\times10^{18}$ cm^{-3}. This estimate is very crude; however, it is consistent with Hall measurements of the sample[15] which give an upper limit for $n=10^{19}$ cm^{-3}. This low density indicates that the nanotubes are semimetallic.[16] The low-temperature upturn of χ_s closely follows a Curie law (solid line, Fig. 2) and is thus a signature of localized spins arising either from localization of the carriers or from impurities. In either case the Curie tail corresponds to 1.3×10^{-5} spins/C atom (1.3×10^{18} localized spins/cm^3), close to our estimate of the number of carriers in the semimetallic phase.

Figure 3(b) (inset) shows the g-factor dependence on θ ($T=300$ K). The g factor varies between $g_\parallel=2.0137$, i.e., when the tubes are parallel to the field $g_\perp=2.0103$ when they are perpendicular and accurately follows[17]

$$g=\sqrt{(g_\parallel\cos\theta)^2+(g_\perp\sin\theta)^2}\approx g_\parallel+(g_\perp-g_\parallel)\sin^2\theta$$
$$=2.0137-0.0034\sin^2\theta.$$

It is instructive to compare the nanotube data with planar graphite. From the rolled graphite nanotube model introduced above, using $T=300$ K and planar graphite g factors, we find

$$g=g_{ab}+\tfrac{1}{2}(g_c-g_{ab})\sin^2\theta=2.0026+0.0230\ \sin^2\theta,$$

where $g_c=2.050$ and $g_{ab}=2.0026$,[12] the factor 1/2 arising from cylindrical geometry. We assumed that the spin diffusion length ξ (the range over which the g factor is averaged) is much larger than the tube diameter, consistent with measurements on polycrystalline graphites.[13] Comparing the model with the tubes we note that whereas in graphite $g_{ab}<g_c$, in the tubes $g_\parallel>g_\perp$. This inversion is similar to the one observed in the static susceptibilities and, as for graphite, probably has the same origin.[14]

The orientationally averaged g factor for the nanotubes, i.e., $g_{ave}=2.012$, is close to the graphitic average $g_{ave}=(g_c+2g_{ab})/3=2.018$, and hence similar to the g factor of polycrystalline graphites for which the crystallite sizes are much smaller than $\xi\sim1$ μm.[13] Consequently, compared with planar graphite the main effect of the tube geometry on the g factors is to reduce the anisotropy; however, the average is not greatly affected. This is related to the graphitic property where the g factor of the carriers is sensitive to the field direction due to band anisotropies,[14] suggesting that the curvature enhances the overlap of the wave functions of neighboring cylindrical sheets.

The temperature dependence of $g_\parallel$ and $g_\perp$ is plotted in Fig. 3(a). Their values increase with decreasing temperature down to 40 K. Since the g shift from the free-electron ($g_e=2.0023$) value is roughly given by $\Delta g\sim\lambda/\Delta$ where λ is the spin-orbit coupling energy and Δ the energy separation of the spin-orbit coupled states, the T dependence of the g shift reflects the T dependence of Δ.[14] For planar graphite a similar increase is observed. However, the decrease in the g shifts and especially the increase in the anisotropy $(g_\parallel-g_\perp)$ for $T<40$ K [Fig. 3(b)] are not expected.

In conventional metals, the conduction-electron spin-resonance (CESR) linewidth (T_1^{-1}) is determined by the Elliott mechanism[18] (spin relaxation due to lattice scattering), and T_1 is related to the resistive scattering time τ_R by $\tau_R=T_1\Delta g^2/\alpha$, where α is a constant in the range 0.1–1.0.[19] A plot of $(T_1\Delta g^2)^{-1}\sim\tau_R^{-1}$ as a function of temperature (Fig. 4) shows that τ_R is of the order of $\sim10^{-13}$ s consistent with typical (graphite) lattice scattering times. The Pauli susceptibility of the nanotubes together with the metallic temperature dependence of τ_R^{-1} suggests that the Elliott mechanism is applicable for this system. From τ_R the intrinsic tube resistivity is estimated: $\rho_{int}=m/ne^2\tau_R\approx10^{-3}$ Ω cm at room temperature, where n is the carrier density above and m is the carrier mass, assuming a free-electron mass and $\alpha=1$. (Note that taking the electron mass of graphite $m^*=m/40$, the intrinsic resistivity of the tubes is even lower.) This value is about an order of magnitude lower than the dc resistivities ρ_{dc} of these films[6] (see also Ref. 20), consistent with the

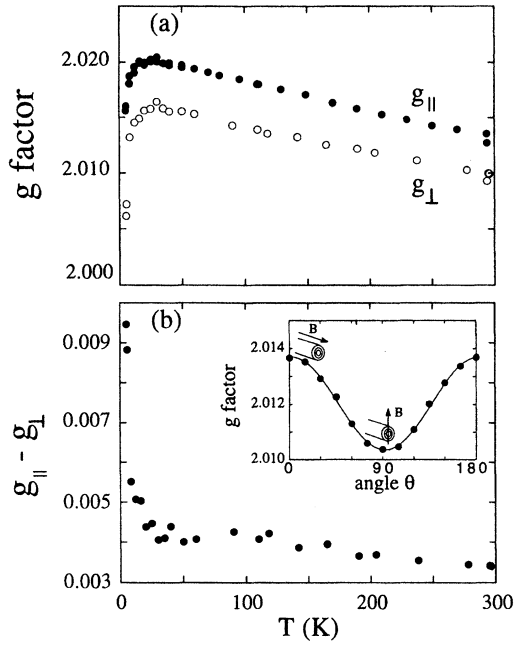

FIG. 3. Nanotube g factors vs temperature, (a) for parallel, $\theta = 0°$(●) and perpendicular, 90°(○) orientations. (b) The anisotropy $g_{\parallel} - g_{\perp}$ vs temperature. (inset) Angular dependence of the g factor of the nanotubes at $T = 300$ K. The fit shown by the solid line corresponds to $g = 2.0137 - 0.0034 \sin^2\theta$.

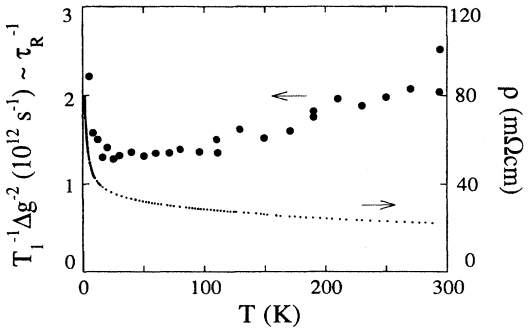

FIG. 4. Inverse resistive scattering times and dc resistivities ρ_{dc} vs temperature. The product $T_1^{-1}\Delta g^{-2}$ (which is proportional to the resistive scattering rate τ_R^{-1}, see text) is compared with ρ_{dc} of the film (Ref. 4).

interpretation that ρ_{dc} is dominated by the intertube contact resistances.[6] Note, however, that ρ_{dc} shows an upturn below 40 K (Fig. 4).

We next demonstrate that the changes which occur below 40 K are consistent with carrier localization effects. Summarizing, the existence of a Curie tail indicates the presence of localized spins. The tail is inconsistent with a narrow-gap semiconductor since it would have a signature of a thermally activated process, i.e., a vanishing of χ_s at low temperatures. Also, since the low-temperature signal does not saturate, it is not likely to be due to dangling bonds (for example, at the tube tips or elsewhere) for which the relaxation times are expected to be long.

The consistency of the number of spins which give rise to the Curie tail (Fig. 2) and the number of carriers at higher temperatures, as well as similar qualitative behavior in the low-temperature dependence of ΔH_{pp} and ρ_{dc},[5] give further evidence of the equivalence of the charge carriers observed at high temperatures and the spin carriers at low temperatures. The fact that g-factor anisotropy not only persists, but even increases below 40 K demonstrates that the spins responsible for the Curie tail must be associated with the nanotubes.

Assuming that the anomalous low-temperature effects are indeed caused by localization, there are several possible localization mechanisms that are consistent with the observations. There may be localized structural defects on the cylindrical sheets,[21] or perhaps specific intercalated impurities which serve as trapping sites for the conduction electrons. Finally, it may be that at low temperatures, the cylindrical sheets of the tubes are no longer exactly coaxial, causing one-dimensional lines of closest distance between neighboring sheets. Nonuniform spacings are indeed observed in several cases[22] (however, see also Ref. 23). Since in graphite the semimetallic properties are quite sensitive to the interlayer spacings (and to the registration of the atoms from one layer to the next), these lines could serve as charge carrier localization sites.

The authors thank L. Zuppiroli, A. Chatelain, and J. P. Ansermet for stimulating discussions.

*Permanent addresss: Laboratório Nacional de Luz Síncrotron (CNPq/MCT), Cx. Postal 6192, 13081-970 Campinas SP, Brazil.

[1] J. P. Lu, Phys. Rev. Lett. **74**, 1123 (1995); J-Y Yi and J. Bernholc, Phys. Rev. B **47**, 1708 (1993); C. T. White, D. H. Robertson, and J. W. Mintmire, Phys. Rev. B **47**, 5485 (1993); N. Hamada, S. Sawada, and A. Oshiyama, Phys. Rev. Lett. **68**, 1579 (1992); R. Saito, M. Fujita, G. Dresselhaus, and M. S. Dresselhaus, Phys. Rev. B **46**, 1804 (1992).

[2] S. Ijima, Nature **354**, 56 (1991).

[3] T. W. Ebbesen and P. M. Ajayan, Nature **358**, 220 (1992); T. W. Ebbesen, Annu. Rev. Mater. Sci. **24**, 235 (1994).

[4] W. A. de Heer, W. S. Bacsa, A. Chatelain, T. Gerfin, R. Humphrey-Baker, L. Forro, and D. Ugarte, Science **268**, 845 (1995).

[5] X. K. Wang *et al.*, J. Mater. Res. **9**, 1578 (1994).

[6] A. P. Ramirez *et al.*, Science **265**, 84 (1994).

[7] Our observations of nanotube bundles directly from the electrode show that they are composed of complex nanotube containing structures with a reasonable, but far from perfect alignment. We suspect that the differences between the processed, aligned tubes and the raw bundles are partly due to local connections between the tubes which are separated in the sonication process. See also Ref. 3 and D. T. Colbert *et al.*, Science **266**, 1218 (1994). Moreover, diamagnetic enhancement is seen in small metal particles in contact with each other; see for example, K. Kimura and S. Bandow, Phys. Rev. B **37**, 4473 (1988).

[8] J. W. McClure, Phys. Rev. **119**, 606 (1960).

[9] J. W. McClure, Phys. Rev. **108**, 612 (1957); R. C. Tatar and S. Rabii, Phys. Rev. B **25**, 4126 (1982), and references therein.

[10] These observations can be compared with those by M. Kosaka

et al., Chem. Phys. Lett. **225**, 161 (1994), who found two ESR lines and considerable asymmetry in their unpurified and also in their oxidation purified nanotube samples.

[11] The low-field to high-field lobe ratio decreases from 1 to 0.7 upon cooling the sample. Absence of a dysonian distortion indicates that the skin depth exceeds the sample thickness (the estimated skin depth is ~ 20 μm at 10 GHz).

[12] G. Wagoner, Phys. Rev. **118**, 647 (1960).

[13] L. S. Singer and G. Wagoner, J. Chem. Phys. **37**, 1812 (1962).

[14] Y. Yafet, in *Solid State Physics*, edited by F. Seitz and D. Turnbull (Academic, New York, 1963), Vol. 14, p. 1.

[15] The Hall coefficient increases from 0.22 cm^3/C at 300 K to 0.44 cm^3/C at 4 K, L. Forro *et al.* (unpublished).

[16] These densities are comparable to graphite [$n \sim 4 \times 10^{18}/cm^3$, D. E. Soule, Phys. Rev. **112**, 708 (1960)] and comparable to values by Song *et al.*, Phys. Rev. Lett. **72**, 697 (1994), obtained from galvanomagnetic measurements on nanotube bundles.

[17] In contrast, no variation in the ESR signal is detected when the sample is rotated in the plane normal to the tube axis as may be expected from geometrical considerations.

[18] R. J. Elliot, Phys. Rev. **96**, 266 (1954).

[19] F. Beneu and P. Monod, Phys. Rev. B **18**, 2422 (1978).

[20] Langer *et al.*, J. Mater. Res. **9**, 927 (1994).

[21] O. Zhou *et al.*, Science **263**, 1744 (1994); T. Ebbesen and K. Tanigaki (private communication).

[22] N. Wang *et al.*, Chem. Phys. Lett. **229**, 587 (1994); M. Liu and J. M. Cowley, Ultramicroscopy **53**, 333 (1994); D. Ugarte (unpublished).

[23] J. C. Charlier and J. Pl Michenaud, Phys. Rev. Lett. **70**, 1958 (1993).